

Diffusion tensor imaging study in Duchenne muscular dystrophy

Ya Fu¹, Yuru Dong², Chao Zhang², Yu Sun¹, Shu Zhang¹, Xuetao Mu², Hong Wang², Weihai Xu³, Shiwen Wu¹

¹Department of Neurology, ²Department of MRI, General Hospital of Chinese People's Armed Police Forces, Beijing 100039, China; ³Department of Neurology, Peking Union Medical College Hospital and Chinese Academy of Medical Science, Beijing 100005, China

Contributions: (I) Conception and design: S Wu, Y Fu, X Mu; (II) Administrative support: H Wang, W Xu, S Wu; (III) Provision of study materials or patients: S Wu, Y Sun, S Zhang; (IV) Collection and assembly of data: Y Dong, C Zhang, Y Sun, S Zhang, X Mu, Y Fu; (V) Data analysis and interpretation: Y Dong, C Zhang, X Mu, Y Fu; (VI) Manuscript writing: All authors; (VII) Final approval of manuscript: All authors.

Correspondence to: Shiwen Wu. Department of Neurology, General Hospital of Chinese People's Armed Police Forces, 69 Yongding Road, Haidian District, Beijing 100039, China. Email: neurowu@gmail.com.

Background: Duchenne muscular dystrophy (DMD) is a progressive muscle disorder associated with an intellectual deficit which is non-progressive. The aim of this study was to investigate brain microstructural changes in DMD and to explore the relationship between such changes and cognitive impairment.

Methods: All participants (12 DMD patients, 14 age-matched healthy boys), intelligence quotients (IQs) [both full (FIQ) and verbal (VIQ)] were evaluated using the Wechsler intelligence scale for children China revised (WISC-CR) edition, and brain gray matter (GM) and white matter (WM) changes were mapped using diffusion tensor imaging (DTI) with fractional anisotropy (FA). The differences between groups were analyzed using the *t*-test and the association of cognition with neuroimaging parameters was evaluated using Pearson's correlation coefficient.

Results: Compared to the normal controls, the DMD group had lower FIQ (82.0±15.39 *vs.* 120.21±16.06) and significantly lower splenium of corpus callosum (CC) FA values (*P*<0.05). Splenium of CC FA was positively correlated with VIQ (*r*=0.588, *P*=0.044).

Conclusions: There were microstructural changes of splenium of CC in DMD patients, which was associated with cognitive impairment.

Keywords: Duchenne muscular dystrophy (DMD); cognitive impairment; diffusion tensor imaging (DTI)

Submitted Feb 22, 2016. Accepted for publication Mar 10, 2016.

doi: 10.21037/atm.2016.03.19

View this article at: <http://dx.doi.org/10.21037/atm.2016.03.19>

Introduction

Duchenne muscular dystrophy (DMD) is an X-linked recessive genetic disorder that affects approximately one in 3,500 male births (1). Mutations within the largest gene in the human genome, the dystrophin gene, block the expression of the functional form of its major protein product, dystrophin (2). Dystrophin is essential in maintaining the structural integrity of muscle membranes during contraction; its absence results in muscle fibre damage, chronic inflammation, and fibrosis (3) leading to progressive muscle weakness and death, generally in the third decade, due to cardiac and pulmonary complications.

Many case reports have suggested the significant

involvement of the central nervous system in DMD. Indeed, Duchenne himself, when characterizing the disorder, commented on the cognitive deficits apparent in some children with DMD (4). Considerable data now indicate that the mean intelligence quotients (IQ) is significantly lower in children with DMD than in the normal population, and a meta-analysis revealed that it is on average one standard deviation below the mean (5). The average IQ of a boy with DMD is 85, and consequently 30% of boys with DMD have an IQ of <70.

The core cognitive deficit in DMD is "limited verbal span" (6). Some researchers have noted that children with DMD have greater difficulty on tests requiring attention to and repetition of verbal material (6-10). This finding

remains consistent regardless of whether children with DMD are compared to normal controls, their siblings, or children with other degenerative muscle diseases. The verbal deficits appear across all intellectual levels (7) while other areas of cognition are generally spared (8). The pathogenesis of cognitive impairment remains unexplained.

Diffusion tensor imaging (DTI), a variant of MRI which measures water diffusion in living brain tissues (11), is uniquely sensitive to changes in white matter (WM) microstructure, including axonal coherence, fibre density, and myelin integrity. One common DTI-derived index of WM microstructure is fractional anisotropy (FA), an indirect scalar measure of the coordinated directionality and coherence of fibres within WM bundles (11,12). Lower FA can also indicate a reduction in the density of WM fibres, a loss in axonal bundle coherence (loss of structural organization), or a variation in membrane permeability to water (13). DTI has been applied to the study of a tremendous variety of complex conditions (14-16) including schizophrenia (17), traumatic brain injury (18), multiple sclerosis (19,20), autism (21), and aging (22). Using DTI, this study sought to investigate brain microstructural changes in patients with DMD and to explore the relationship between such changes and cognitive dysfunction.

Materials and methods

Participants

This study recruited 12 patients [age 9.14 ± 2.52 years (range, 6–13)] with a diagnosis of DMD (confirmed by genetic testing or muscle biopsy) from the DMD Multidisciplinary Outpatient Clinic of CAPF General Hospital, and 14 healthy volunteers [age 9.39 ± 2.99 years (range, 6–14)]. Those who had a medical or surgical history of potential impact on neurocognitive functioning (e.g., head injury), were not contactable, or whose parents refused to consent were excluded. Both groups (DMD and control) had similar mean age, handedness (all right-handed), and level of education. After the study protocol was approved by the Armed Police General Hospital review board, written informed consent was obtained from all the parents according to the Declaration of Helsinki.

Cognitive measures

All subjects underwent a Wechsler intelligence scale for children China revised (WISC-CR) test performed by a

trained neuropsychologist.

Image acquisition

Conventional MRI examination was performed in all subjects on a 3.0 T MR scanner (Magnetom TRIO TIM, Siemens Medical Systems, Erlangen, Germany) with a SENSE 8-channel head coil, and the imaging sequences included an axial T1-weighted fast low-angle shot sequence [repetition time (TR)/echo time (TE) = 200/2.46 ms, slice thickness = 5 mm, intersection gap = 1.5 mm, slice number = 19, field of view (FOV) = 220 mm × 220 mm], sagittal and axial T2-weighted turbo spin echo sequences (TR/TE = 4,000/113 ms, slice thickness = 5 mm, intersection gap = 1.5 mm, slice number = 19, FOV = 220 mm × 220 mm), and an axial fluid-attenuated inversion recovery sequence (TR/TE = 8,000/87 ms, inversion time = 2,000 ms, slice thickness = 5 mm, intersection gap = 1.5 mm, slice number = 19, FOV = 320 mm × 224 mm). Diffusion tensor images were acquired using a spin-echo diffusion-weighted echo-planar imaging sequence parallel to the anterior-posterior commissure line (TR/TE = 4,400/93 ms, slice thickness = 4 mm, number of slices = 32, FOV = 220 mm × 220 mm, matrix = 128 × 128). MRI images were obtained from 20 non-collinear directions with a b value of $1,000 \text{ s/mm}^2$, scan time = 6.24 min.

ROI placement

Two neuroradiologists separately outlined regions of interest (ROIs) on two Siemens Syngo parallel processing workstations (Siemens Medical Solutions, Erlangen, Germany) using the commercially available software Neuro3D. To ensure the reliability of ROI-based DTI parameters, ROI placement was carried out by both observers on two separate occasions. The information about the first ROI placement was not available during the second assessment, and the investigator was blinded to the other observer's evaluation. We selected 16 different ROIs in locations with different FA. The locations were commonly used in DTI studies and easily visualized and delineated on DTI color maps. Predetermined circular single ROIs were manually placed on color maps at the following anatomic locations: parietal lobe WM, frontal lobe WM, genu of corpus callosum (CC), splenium of CC, caput nuclei caudati, anterior cingulate (AC), posterior cingulate (PC), lenticular nucleus, anterior limb of the internal capsule (ICAL), posterior limb of the internal capsule (ICPL),

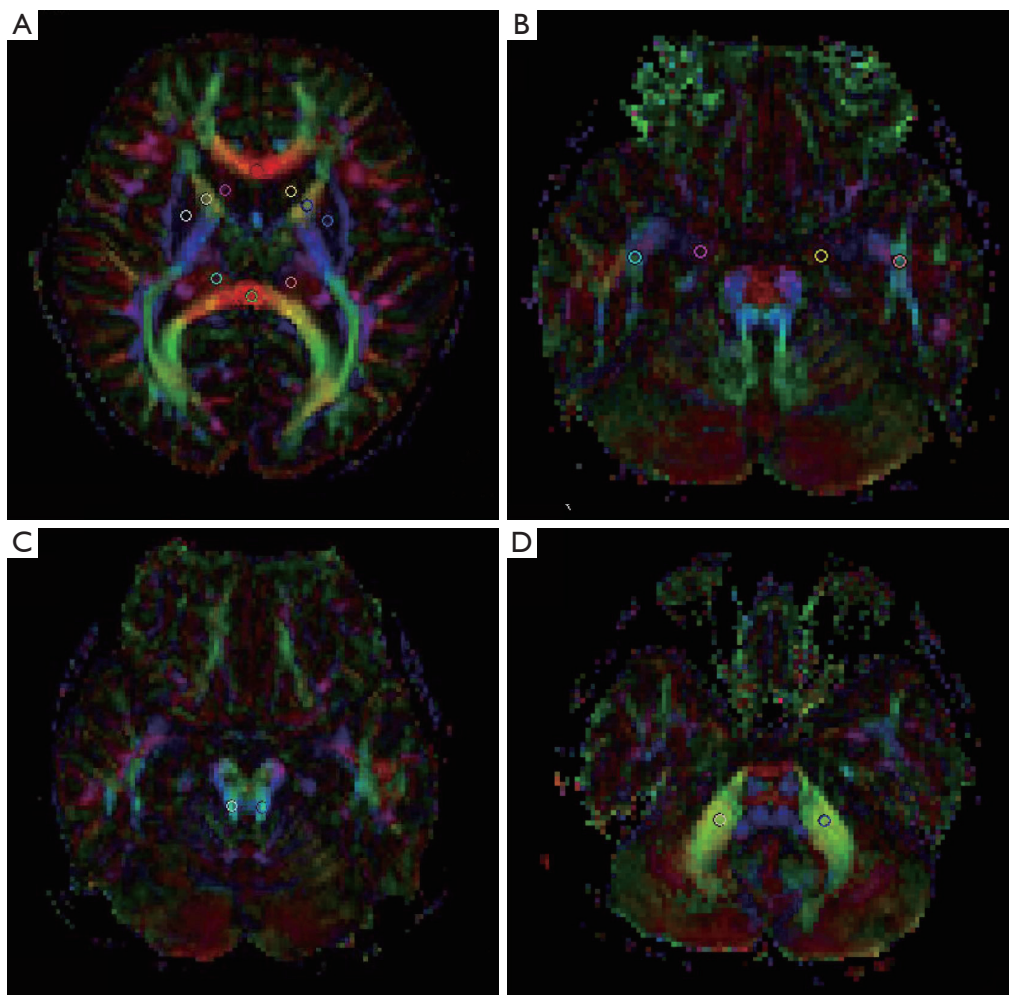


Figure 1 Region of interest placement for DTI analysis. The circle indicates the location and size of the ROI. (A) Genu of corpus callosum, splenium of corpus callosum, caput nuclei caudati, lenticular nucleus, anterior limb of ICAL, posterior limb of ICPL, and Th; (B) temporal lobe WM and CgH; (C) SCP; (D) MCP. DTI, diffusion tensor imaging; ROI, outlined regions of interest; ICAL, internal capsule; ICPL, internal capsule; Th, thalamus; WM, white matter; CgH, cingulum in the hippocampus; SCP, superior cerebellar peduncle; MCP, middle cerebellar peduncle.

thalamus (Th), occipital lobe WM, temporal lobe WM, cingulum in the hippocampus (CgH), superior cerebellar peduncle (SCP), and middle cerebellar peduncle (MCP). As illustrated in *Figure 1*, with the exception of the CC, all of the ROIs were positioned bilaterally and three voxels in size.

Statistical analyses

The statistical analyses were performed using the SPSS 19 software package for Windows (Chicago, IL, USA). Age was compared between groups using the independent

samples *t*-test. Differences in FA for a ROI between the patient and control groups were also assessed using the independent samples *t*-test. The relationship between diffusion parameters and clinical outcome measures was assessed using Pearson's correlation coefficient. Differences were considered significant for $P < 0.05$.

Results

Age was similar between the two groups, and IQ was significantly lower in DMD patients than in healthy individuals [82.00 ± 15.39 (range, 66–111) *vs.* 120.21 ± 16.06

(range, 98–137)].

Compared with the 14 subjects in the normal control group, no gross structural abnormalities had detected in conventional MRI examination, but the DMD group had significantly reduced splenium of CC FA values (*Table 1*). However, no statistically significant between-group differences were apparent in the parietal lobe WM, frontal lobe WM, genu of CC, caput nuclei caudati, AC, PC, lenticular nucleus, ICAL, ICPL, Th, occipital lobe WM, temporal lobe WM, cingulum in the CgH, SCP, MCP.

In the DMD group, interestingly, there was a significant correlation between FA of the splenium of CC and verbal intelligence quotient (VIQ; $t=0.588$, $P=0.044$) but not between FA of the splenium of CC and the full intelligence quotient (FIQ) (*Figure 2*).

Discussion

Few studies have assessed the potential correlation between microstructural damage and altered cognition in DMD. Comparing the cognitive profile and brain DTI between two groups (a DMD group and normal group), we demonstrated the relationship of reduced IQ to microstructural abnormalities in the splenium of CC in DMD patients. Interestingly, VIQ impairment was correlated with splenium of CC damage.

Previous studies have shown that DMD patients with identifiable brain abnormalities may also show cognitive impairment. In the study by Septien *et al.* (23) of 15 DMD patients, aged 4–16 years, CT scans showed slight cortical atrophy with minimal dilation of the ventricles (interpreted as atrophy of the WM) in 9 patients with an average IQ of 81, and normal CT scans in 6 patients with an average IQ of 90. However, this difference was not statistically significant. In contrast, al-Qudah *et al.* (24) found no correlation between MRI findings and verbal intelligence scores for four patients, two of whom were found to have mild atrophy (i.e., dilated lateral ventricles, CSF spaces, and cerebral sulci). Similarly, a MRI study by Bresolin and colleagues found no focal or generalized changes, but their sample was very small ($n=4$) (25).

Brain autopsy studies have found a range of abnormalities in the brains of DMD patients, including pathological findings of neuronal loss, heterotopias, gliosis, neurofibrillary tangles, Purkinje cell loss, dendritic abnormalities (length, branching and intersections), disordered architecture, astrocytosis, and perinuclear vacuolation (26–29). Yoshioka *et al.* studied 30 DMD patients and found slight cortical

atrophy in 67% of them, slight ventricular dilation (i.e., enlargement of inter-hemispheric cisterns and sulci of 3–5 mm) in 60%, and cortical atrophy in 30%, although clear signs of atrophy were only observed in older and more physically disabled patients (30). However the brain autopsy results, and more recently the brain imaging results, on DMD patients have not been consistent (31). These alterations in brain structure impact brain function, and likely underlie the cognitive deficits seen in children with DMD. Correlation between structural abnormality and functional IQ impairment has yet to be clearly established.

DTI, a variant of MRI which measures water diffusion in living brain tissues (11), is uniquely sensitive to WM microstructure. Using DTI, we found that the splenium of CC is changed in DMD patients. The CC is the brain's largest WM structure and its more than 200 million fibres play an integrative role by facilitating the coordinated and rapid transfer of information involved in sensorimotor, attention, language, and other cognitive processes between contralateral, homologous cortical regions (32–34). The splenium fibres connect occipital and parietal cortices, as well as inferior and medial temporal regions, which have been suggested to play a role in language processing (35,36). Accordingly, our study showed a significantly positive correlation between VIQ values and FA in splenium of CC in DMD patients. Axonal loss, inflammation, oedema, gliosis and Wallerian degeneration may all potentially contribute to these FA changes, but direct pathological correlation with DTI changes is lacking. The changes may be potentially important clinically and need to be studied further.

Children with DMD have dystrophin gene deletions. Firstly, dystrophin is present in many cells throughout the body, including CNS neurons, glia, and vascular endothelial cells (which are regulated by the M-promotor). Dystrophin has a great many interactions with a variety of proteins of the extracellular matrix, plasma membrane, cytoskeleton, and distinct intracellular compartments. Therefore, the lack of dystrophin expression may contribute to the WM changes. Secondly, since dystrophin mainly exists in the cerebral cortex, hippocampus, and cerebellar neurons, its absence may result in changes in WM tracts connected to homologous brain gray matter (GM). Doorenweerd *et al.* using voxel-based morphometry found that DMD patients have a significantly smaller occipital cortex and significantly lower WM FA in the occipital lobe (37). Thirdly, during neural development, dystrophin is expressed within the neural tube and selected areas of the embryonic and postnatal neuraxis, and may regulate distinct

Table 1 Comparison of brain region FA values between the DMD group and healthy controls (mean \pm SD)

Location	DMD	Controls	<i>t</i>	P
Parietal lobe WM				
Left	0.482 \pm 0.063	0.458 \pm 0.051	1.081	0.291
Right	0.463 \pm 0.063	0.430 \pm 0.046	1.523	0.141
Frontal lobe WM				
Left	0.407 \pm 0.093	0.380 \pm 0.079	0.803	0.430
Right	0.417 \pm 0.087	0.378 \pm 0.070	1.259	0.220
Genu of corpus callosum	0.775 \pm 0.066	0.801 \pm 0.093	-0.805	0.429
Splenium of corpus callosum	0.790 \pm 0.123	0.883 \pm 0.047	-2.441	0.029*
Caput nuclei caudati				
Left	0.132 \pm 0.030	0.154 \pm 0.050	-1.279	0.213
Right	0.138 \pm 0.031	0.148 \pm 0.053	-0.572	0.573
Occipital lobe WM				
Left	0.653 \pm 0.074	0.636 \pm 0.074	0.576	0.570
Right	0.657 \pm 0.068	0.675 \pm 0.101	-0.523	0.606
Anterior cingulate				
Left	0.172 \pm 0.045	0.166 \pm 0.057	0.294	0.7711
Right	0.180 \pm 0.052	0.179 \pm 0.069	0.053	0.958
Posterior cingulate				
Left	0.178 \pm 0.039	0.183 \pm 0.038	-0.375	0.717
Right	0.179 \pm 0.033	0.192 \pm 0.032	-1.022	0.317
Lenticular nucleus				
Left	0.121 \pm 0.028	0.112 \pm 0.027	-0.791	0.437
Right	0.114 \pm 0.027	0.125 \pm 0.024	-1.128	0.270
Posterior limb of internal capsule				
Left	0.761 \pm 0.033	0.742 \pm 0.072	0.891	0.384
Right	0.787 \pm 0.023	0.752 \pm 0.079	1.592	0.132
Anterior limb of internal capsule				
Left	0.626 \pm 0.090	0.624 \pm 0.088	0.071	0.944
Right	0.635 \pm 0.068	0.606 \pm 0.094	0.881	0.387
Thalamus				
Left	0.272 \pm 0.064	0.293 \pm 0.055	-0.874	0.391
Right	0.284 \pm 0.048	0.272 \pm 0.055	0.589	0.562
Temporal lobe WM				
Left	0.464 \pm 0.073	0.497 \pm 0.090	-1.010	0.323
Right	0.495 \pm 0.080	0.444 \pm 0.086	1.564	0.131
Hippocampus				
Left	0.163 \pm 0.042	0.155 \pm 0.037	0.516	0.611
Right	0.148 \pm 0.044	0.154 \pm 0.036	-0.413	0.683
Superior cerebellar peduncle				
Left	0.752 \pm 0.043	0.753 \pm 0.072	-0.015	0.988
Right	0.761 \pm 0.040	0.763 \pm 0.070	-0.135	0.894
Middle cerebellar peduncle				
Left	0.738 \pm 0.059	0.760 \pm 0.088	-0.923	0.365
Right	0.774 \pm 0.075	0.797 \pm 0.060	-0.874	0.391

*, P<0.05. FA, fractional anisotropy; DMD, Duchenne muscular dystrophy; WM, white matter.

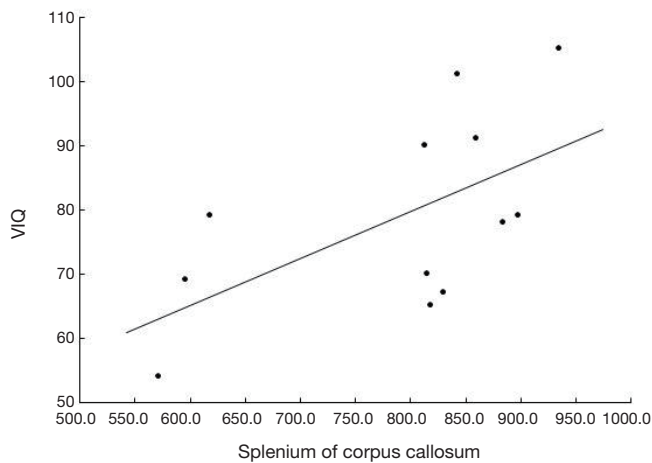


Figure 2 Correlation between VIQ and FA value in the splenium of corpus callosum in DMD. VIQ, verbal intelligence quotients score; FA, fractional anisotropy; DMD, Duchenne muscular dystrophy.

aspects of neurogenesis, neuronal migration, and cellular differentiation. Further research is needed to delineate the exact mechanism of microstructural brain changes in DMD.

One limitation of this study was the use of manual ROIs to measure FA in WM tracts. ROIs are subject to intra-rater and inter-rater variability in placement, and do not cover the entire fibre pathway. Further improvements in signal-to-noise ratios continue to be required for more precise calculation of anisotropy measures and more accurate WM fibre tracking. Voxel-based morphometry and further DTI analysis will be used in our future studies.

Conclusions

Our study has shown that there were microstructural changes of splenium of CC in DMD patients, which was associated with cognitive impairment.

Acknowledgements

Funding: This work was supported by Capital characteristic clinic project (grant No. Z151100004015025). The funders had no role in study design, data collection and analysis, decision to publish, or preparation of the manuscript.

Footnote

Conflicts of Interest: The authors have no conflicts of interest to declare.

References

- Emery AE. Population frequencies of inherited neuromuscular diseases--a world survey. *Neuromuscul Disord* 1991;1:19-29.
- Hoffman EP, Brown RH Jr, Kunkel LM. Dystrophin: the protein product of the Duchenne muscular dystrophy locus. *Cell* 1987;51:919-28.
- Wallace GQ, McNally EM. Mechanisms of muscle degeneration, regeneration, and repair in the muscular dystrophies. *Annu Rev Physiol* 2009;71:37-57.
- Duchenne GB. Recherches sur la paralysie musculaire pseudohyper trophique, ou paralysie myo-sclerosique. *Clin Orthop Relat Res* 1965;39:3-5.
- Cotton S, Voudouris NJ, Greenwood KM. Intelligence and Duchenne muscular dystrophy: full-scale, verbal, and performance intelligence quotients. *Dev Med Child Neurol* 2001;43:497-501.
- Hinton VJ, De Vivo DC, Fee R, et al. Investigation of Poor Academic Achievement in Children with Duchenne Muscular Dystrophy. *Learn Disabil Res Pract* 2004;19:146-54.
- Hinton VJ, De Vivo DC, Nereo NE, et al. Poor verbal working memory across intellectual level in boys with Duchenne dystrophy. *Neurology* 2000;54:2127-32.
- Hinton VJ, De Vivo DC, Nereo NE, et al. Selective deficits in verbal working memory associated with a known genetic etiology: the neuropsychological profile of duchenne muscular dystrophy. *J Int Neuropsychol Soc* 2001;7:45-54.
- Wicksell RK, Kihlgren M, Melin L, et al. Specific cognitive deficits are common in children with Duchenne muscular dystrophy. *Dev Med Child Neurol* 2004;46:154-9.
- Hinton VJ, Fee RJ, Goldstein EM, et al. Verbal and memory skills in males with Duchenne muscular dystrophy. *Dev Med Child Neurol* 2007;49:123-8.
- Beaulieu C. The basis of anisotropic water diffusion in the nervous system - a technical review. *NMR Biomed* 2002;15:435-55.
- Mori S, Zhang J. Principles of diffusion tensor imaging and its applications to basic neuroscience research. *Neuron* 2006;51:527-39.
- Beaulieu C, Allen PS. Water diffusion in the giant axon of the squid: implications for diffusion-weighted MRI of the nervous system. *Magn Reson Med* 1994;32:579-83.
- Horsfield MA, Jones DK. Applications of diffusion-weighted and diffusion tensor MRI to white matter diseases - a review. *NMR Biomed* 2002;15:570-7.

15. Ciccarelli O, Catani M, Johansen-Berg H, et al. Diffusion-based tractography in neurological disorders: concepts, applications, and future developments. *Lancet Neurol* 2008;7:715-27.
16. Assaf Y, Pasternak O. Diffusion tensor imaging (DTI)-based white matter mapping in brain research: a review. *J Mol Neurosci* 2008;34:51-61.
17. Kubicki M, McCarley R, Westin CF, et al. A review of diffusion tensor imaging studies in schizophrenia. *J Psychiatr Res* 2007;41:15-30.
18. Maller JJ, Thomson RH, Lewis PM, et al. Traumatic brain injury, major depression, and diffusion tensor imaging: making connections. *Brain Res Rev* 2010;64:213-40.
19. Inglese M, Bester M. Diffusion imaging in multiple sclerosis: research and clinical implications. *NMR Biomed* 2010;23:865-72.
20. Filippi M, Agosta F. Imaging biomarkers in multiple sclerosis. *J Magn Reson Imaging* 2010;31:770-88.
21. Lange N, Dubray MB, Lee JE, et al. Atypical diffusion tensor hemispheric asymmetry in autism. *Autism Res* 2010;3:350-8.
22. Westlye LT, Walhovd KB, Dale AM, et al. Life-span changes of the human brain white matter: diffusion tensor imaging (DTI) and volumetry. *Cereb Cortex* 2010;20:2055-68.
23. Septien L, Gras P, Borsotti JP, et al. Mental development in Duchenne muscular dystrophy. Correlation of data of the brain scanner. *Pediatrie* 1991;46:817-9.
24. al-Qudah AA, Kobayashi J, Chuang S, et al. Etiology of intellectual impairment in Duchenne muscular dystrophy. *Pediatr Neurol* 1990;6:57-9.
25. Bresolin N, Castelli E, Comi GP, et al. Cognitive impairment in Duchenne muscular dystrophy. *Neuromuscul Disord* 1994;4:359-69.
26. Rosman NP, Kakulas BA. Mental deficiency associated with muscular dystrophy. A neuropathological study. *Brain* 1966;89:769-88.
27. Rosman NP. The cerebral defect and myopathy in Duchenne muscular dystrophy. A comparative clinicopathological study. *Neurology* 1970;20:329-35.
28. Jagadha V, Becker LE. Brain morphology in Duchenne muscular dystrophy: a Golgi study. *Pediatr Neurol* 1988;4:87-92.
29. Itoh K, Jinnai K, Tada K, et al. Multifocal glial nodules in a case of Duchenne muscular dystrophy with severe mental retardation. *Neuropathology* 1999;19:322-27.
30. Yoshioka M, Okuno T, Honda Y, et al. Central nervous system involvement in progressive muscular dystrophy. *Arch Dis Child* 1980;55:589-94.
31. Dubowitz V, Crome L. The central nervous system in Duchenne muscular dystrophy. *Brain* 1969;92:805-8.
32. Walterfang M, Malhi GS, Wood AG, et al. Corpus callosum size and shape in established bipolar affective disorder. *Aust N Z J Psychiatry* 2009;43:838-45.
33. Doron KW, Gazzaniga MS. Neuroimaging techniques offer new perspectives on callosal transfer and interhemispheric communication. *Cortex* 2008;44:1023-9.
34. Tomasch J. Size, distribution, and number of fibres in the human corpus callosum. *Anat Rec* 1954;119:119-35.
35. Gadea M, Marti-Bonmati L, Arana E, et al. Corpus callosum function in verbal dichotic listening: inferences from a longitudinal follow-up of Relapsing-Remitting Multiple Sclerosis patients. *Brain Lang* 2009;110:101-5.
36. Corbetta M, Shulman GL. Control of goal-directed and stimulus-driven attention in the brain. *Nat Rev Neurosci* 2002;3:201-15.
37. Doorenweerd N, Straathof CS, Dumas EM, et al. Reduced cerebral gray matter and altered white matter in boys with Duchenne muscular dystrophy. *Ann Neurol* 2014;76:403-11.

Cite this article as: Fu Y, Dong Y, Zhang C, Sun Y, Zhang S, Mu X, Wang H, Xu W, Wu S. Diffusion tensor imaging study in Duchenne muscular dystrophy. *Ann Transl Med* 2016;4(6):109. doi: 10.21037/atm.2016.03.19